Available online at www.sciencedirect.com
SCIENCE DIRECT
Journal of Catalysis 235 (2005) 10–17
JOURNAL OF CATALYSIS
www.elsevier.com/locate/jcat

TiO_2 nanotube-supported ruthenium(III) hydrated oxide: A highly active catalyst for selective oxidation of alcohols by oxygen

Dmitry V. Bavykin [a,*], Alexei A. Lapkin [a], Pawel K. Plucinski [a], Jens M. Friedrich [b], Frank C. Walsh [b]

[a] *Catalysis and Reaction Engineering Group, Department of Chemical Engineering, University of Bath, Bath, BA2 7AY, UK*
[b] *Electrochemical Engineering Group, School of Engineering Sciences, University of Southampton, Highfield, Southampton SO17 1BJ, UK*

Received 31 May 2005; revised 11 July 2005; accepted 12 July 2005

Available online 18 August 2005

Abstract

Ruthenium(III) hydrated oxide was deposited onto the surface of TiO_2 nanotubes via ion exchange followed by alkali treatment. The catalytic activity of Ru(III)/TiO_2 catalyst for the selective oxidation of alcohols by oxygen was studied in a continuous multichannel, compact reactor. It was found that the activity of Ru(III)/TiO_2 (turnover frequency [TOF] $\leqslant 450\ h^{-1}$) is greater than that of a recently reported Ru(III)/Al_2O_3 catalyst (TOF $= 335\ h^{-1}$), and that the ruthenium loading could exceed 8 wt% without any significant loss of specific catalytic activity. High-resolution transmission electron microscopy and X-ray diffraction data show that ruthenium is highly dispersed on both the inner and the outer surfaces of the mesoporous TiO_2 nanotubes with the diameter of nanoparticles between 1.2 and 2.4 nm, and is easily accessible by reactant molecules.

Keywords: $Ru(OH)_3$; $RuO_x \cdot nH_2O$; Nanostructures; Titration; Deactivation; Nanotubular TiO_2

1. Introduction

The growing demand for fine chemicals in the pharmaceutical and fine chemicals industries, and increasingly stringent ecological standards, require new technologies for liquid phase selective oxidation of alcohols with air or molecular oxygen using heterogeneous catalysts [1]. Specific aspects of oxidation by air or oxygen, including control of selectivity, high exotherm, and potential risk of explosion, stimulate the design of new reactors with intensive mass/heat transfer and the development of active stable heterogeneous catalysts. The millimetre-scale packed-bed reactors have several integrated functionalities; that is, static mixers, reaction, and heat transfer are characterised by (i) efficient heat transfer [2] and mass transfer, (ii) the possibility of operation in the continuous flow regime, (iii) simple scale-up. At the same time, millimetre-scale reactors do not suffer from the drawbacks of the micron-scale reactors, namely channel plugging by solid impurities or products with low solubility, impractically low throughputs, and high cost. The millimetre-scale reactors are expected to be very useful in industries requiring rapid product development and variability of production volumes, and they are very convenient tools for investigating catalytic activity of heterogeneous catalysts in three-phase reactions [3].

Ruthenium(III)-hydrated oxide [4] is a promising new catalyst for selective oxidation of alcohols in the liquid phase by molecular oxygen, characterised by high activity and selectivity. For the successful application of this catalyst in industry, optimisation of the support is required to provide high loading and high dispersion of the active centres. So far, the most active catalyst reported has been ruthenium deposited on γ-Al_2O_3 [5]. In this case, however, the catalyst loading could not exceed 1.4 wt%, indicating a limited number of Ru^{3+} adsorption sites on alumina. The

* Corresponding author. Fax: +44-1225-385713.
E-mail address: D.V.Bavykin@bath.ac.uk (D.V. Bavykin).

0021-9517/$ – see front matter
doi:10.1016/j.jcat.2005.07.012

maximum catalyst loading of 17 wt% was achieved for an appatite-based ruthenium catalyst prepared by stoichiometric ion exchange [6]. However, incorporation of ruthenium inside the microporous channels of an ion-exchangeable hydroxyappatite results in deterioration of the catalyst performance. A recent approach for controlling the localisation of ruthenium in hydroxyappatite used a promoting (sacrificial) metal [7].

Nanotubular titanium dioxide, produced by the alkali hydrothermal treatment, is a novel and intensively studied material characterised by a mesopore-range internal diameter (ca. 4–10 nm) and a unique combination of physicochemical properties [8–11]. This material shows promise for a variety of applications, including catalysis [12,13] and photocatalysis [14,15]. The high cation exchange capacity [9,16] of TiO_2 nanotubes should enable high loading of an active catalyst with even distribution and high dispersion. The open mesoporous morphology [17] of the nanotubes, absence of micropores, and high specific surface area should facilitate transport of reagents during a catalytic reaction. The semiconducting properties of TiO_2 nanotubes [18,19] may result in strong electronic interaction between the support and a catalyst, which could improve catalytic performance in redox reactions.

In this paper, we explore the possibility of using TiO_2 nanotubes as a support for ruthenium-hydrated oxide catalyst. We study the effect of Ru loading on the catalyst, and evaluate the catalytic activity of ruthenium-hydrated oxide catalyst deposited on to the TiO_2 nanotubes in the reaction of selective oxidation of alcohols with oxygen in the continuous compact multichannel reactor.

2. Experimental

2.1. Reagents

Titanium dioxide, anatase (TiO_2), sodium hydroxide (NaOH), sulfuric acid (H_2SO_4), hydrochloric acid (HCl), ruthenium(III) chloride hydrate ($RuCl_3{\cdot}nH_2O$), di-dodecyl-di-methylammonium chloride ($(C_{12}H_{25})_2(CH_3)_2NCl$) pure grate, and toluene HPLC grade were obtained from Aldrich and used without further purification.

2.2. Preparation of Ru(III)/TiO_2 nanotubes

The preparation of TiO_2 nanotubes was based on the alkali hydrothermal transformation [20]. Here 20 g of titanium dioxide was added to 300 mL 10 mol NaOH solution and heated for 22 h at 413 K. The white, powdery TiO_2 was thoroughly washed with water, then with 0.05 M H_2SO_4, followed by vacuum-drying at 80 °C. The ruthenium(III)-hydrated oxide was deposited onto TiO_2 nanotubes by consecutive exchange of protons by Ru^{3+} ions, followed by formation of hydrated oxide during the alkali treatment. A given amount of $RuCl_3{\cdot}nH_2O$ (25–200 mg) was dissolved in 25 mL of water with addition of 100 µL of 37 wt% HCl. Then 2 g of nanotubular TiO_2 powder was added and vigorously stirred for 30 min at 25 °C. During this process, the dark-brown colour of the solution turned white, and white TiO_2 turned grey. The obtained powder was filtered and washed with a large amount of demineralised water. The amount of Ru^{3+} in the remaining solution was analysed using atomic absorption spectroscopy (Perkin Elmer). The dark powder was placed in a 100-mL beaker, and 50 mL water was added. Then, under vigorous stirring, 1 M of NaOH was slowly added until the solution reached pH 10. The colour of the produced powder varied from light green to black depending on the catalyst loading. The solids were then filtered and washed with water, then dried in vacuum at 80 °C for 2 h.

2.3. Sample characterisation

Transmission electron microscope (TEM) images were obtained using a JEOL 3010-TEM. Scanning electron microscope (SEM) images were obtained with a JEOL 6500 FEG-SEM. X-ray diffraction (XRD) patterns were recorded using a Bruker AXS D8 Discover, with Cu-K_α radiation ($\lambda = 0.154$ nm) and a graphite monochromator in the 2θ range 20°–50°. The BJH pore size distribution of the samples was measured, using nitrogen adsorption, on a Micromeritics ASAP 2010 instrument.

2.4. Catalytic experiments

The catalytic activity of the Ru(III)/TiO_2 samples was determined in the reaction of benzyl alcohol oxidation with oxygen performed in a continuous-flow compact multichannel reactor with integrated gas/liquid static mixer. Details of the reactor setup are published elsewhere [3]. The reactor channels (100 mm long, 3×3 mm^2 cross-section) were packed with ca. 0.8 g of a catalyst sample and operated in horizontal flow mode. Prepared powders of TiO_2 nanotubes with supported ruthenium-hydrated oxide were used without sieving. Benzyl alcohol was dissolved in toluene (1 M) and pumped through the reactor at a 2 mL min^{-1} flow rate. The oxygen flow rate was varied between 0 and 20 mL (STP) min^{-1}. The operating pressure was 800 kPa (8 bar), with a temperature of 390 K. For the oxygen flow rate equal to 7.2 mL (STP) min^{-1}, the pressure drop in the reactor for the newly packed catalyst slowly increased over 1 h from 0.85 bar to 1.15 bar, due to the rearrangement of catalyst particles; the pressure drop then stabilised after 1 h. The flow inside the reactor was turbulent and may be considered a dispersed plug flow of reactants with different residence times for the gas and liquid phases. The liquid samples were collected in the outlet of the reactor and analysed without dilution or derivatisation using gas chromatography (Varian CP3800).

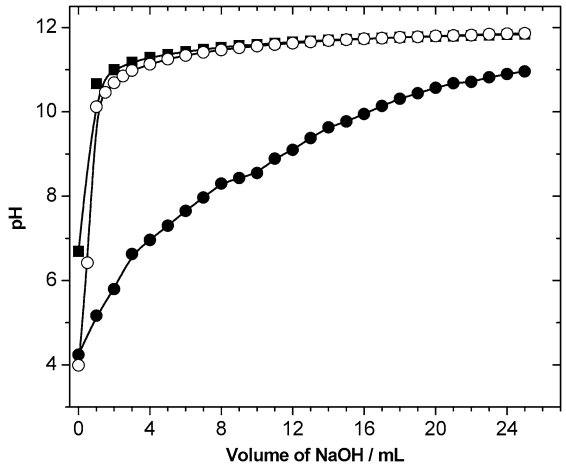

Fig. 1. Titration curves of TiO_2 nanotubes (●), TiO_2 Degussa P25 (○) and blank experiment with distilled water (■), by 0.05 M NaOH. Both TiO_2 powders were washed with 0.1 M HCl before titration. Weight of sample is 0.1 g; initial volume is 25 mL, temperature 298 K.

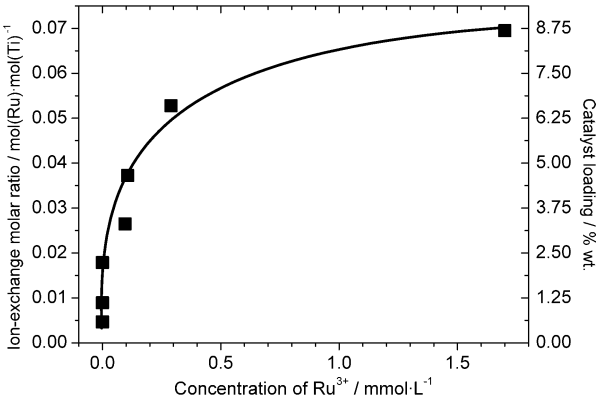

Fig. 2. Isotherm of Ru(III) adsorption onto suspension of TiO_2 nanotubes in water. Temperature is 298 K.

3. Results and discussion

3.1. Deposition of Ru onto TiO_2 nanotubes

Nanotubular "titanium dioxide" is actually a protonated form of a layered titanic acid. The exact crystal structure of the nanotubes is a matter of current dispute; it probably corresponds either to the layered titanate $H_2Ti_3O_7$ [21], which has a monoclinic structure with stepwise layers of three lengths in each step, or to $H_2Ti_2O_4(OH)_2$ [16], in which the unit cell has an orthorhombic symmetry. The nanotube walls have a multilayered structure in which protons occupy positions on either side of the wall surface (convex and concave), as well as in the interstitial cavities between the layers of the nanotube walls. The gap between the layers is 0.73 nm and is not accessible to nitrogen gas molecules [17]. However, protons and cations from aqueous solutions (H^+, Me^{n+}) could easily be exchanged between protons in the nanotube wall, according to the following equation:

$$x\mathrm{Me}^{n+} + \mathrm{H_2Ti_3O_7} \rightarrow \mathrm{Me}_x\mathrm{H}_{2-x}\mathrm{Ti_3O_7}^{x(n-1)+} + x\mathrm{H}^+. \quad (1)$$

Fig. 1 shows the titration curve of nanotubular TiO_2 suspended in water by solution of sodium hydroxide. The shape of the curve corresponds to the titration of a weak diprotic acid by a strong base [22]. Analysis of this curve reveals two plateaus and two endpoints at the following volumes of added NaOH: 3.5 and 16.8 mL. The value of ion-exchange capacity, calculated as the molar ratio of the number of mol of ion-exchanged Na^+ to the number of mol of titanium in the nanotube for the last endpoint, is ca. 0.67. This value suggests that both protons in the nanotubular $H_2Ti_3O_7$ could be successfully substituted by sodium ions.

Transition metal cations could also readily exchange protons in TiO_2 nanotubes, but with smaller ion-exchange ratios. Fig. 2 shows the isotherm of Ru(III) adsorption onto the TiO_2 nanotubes. To obtain this curve, the amount of Ru(III) remaining in solution after the ion exchange with TiO_2 nanotubes was measured and subtracted from the amount of ruthenium in the initial solution. One can see that at small Ru loadings (up to 2.75 wt%), the ion exchange is almost complete, resulting in a very low residual concentration of Ru(III) in solution. Further addition of ruthenium salt establishes a distribution of Ru(III) between the aqueous solution and the nanotubes. It is interesting to note that at certain amount of added ruthenium (the value of catalyst loading corresponding to 3–5 wt%), the colour of the solution after filtration of TiO_2 nanotubes is greenish-blue, indicating possible formation of aqueous Ru(II) through disproportionation of Ru(III) to Ru(II) and Ru(IV). This solution undergoes further oxidation to Ru(III). This demonstrates that during ion exchange the redox reaction of ruthenium could occur.

Aqueous solution of ruthenium(III) chloride represents an intricate mixture of different aqua, hydroxo, and chloride complexes of Ru(III) and Ru(IV) [23,24]. Some of these species occur in the cationic aqueous form and possibly could become attached to the surface of the negatively charged TiO_2 nanotubes. The ionic radius of the hypothetic Ru^{3+} ion is 0.082 nm, whereas the size of the chloro-aqua complexes is ca. 0.5 nm [24,25]. Therefore, only isolated Ru^{3+} ions, and not complex cations, would fit into the interstitial cavity between the layers in the TiO_2 nanotube wall. Knowing that chloride and aqua ligands are very labile [24] and can be easily substituted, one can assume that ion exchange of protons to ruthenium(III) ions in TiO_2 nanotubes is accompanied by the decomposition of chloride-aqua complex and incorporation of ruthenium atoms into the lattice of $\mathrm{Ru}_x\mathrm{H}_{2-x}\mathrm{Ti_3O_7}^{2x+}$ nanotubes. This could explain the large value of observed ion-exchange molar ratio for ruthenium (see Fig. 2), which corresponds to $x \approx 0.2$ in Eq. (1).

Incorporation of ruthenium ions from solution into the lattice of nanotubes is accompanied by a change in the absorption spectrum (see Fig. 3a). The spectrum of "$RuCl_3$" in presence of HCl in aqueous solution exhibits two characteristic bands at 392 and 458 nm and is similar to the spectrum of aquapentachlororuthenate [26]. Addition of colloidal TiO_2 nanotubes to this solution with molar excess

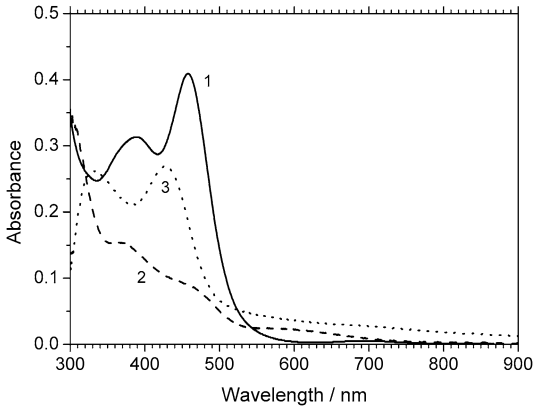

(a)

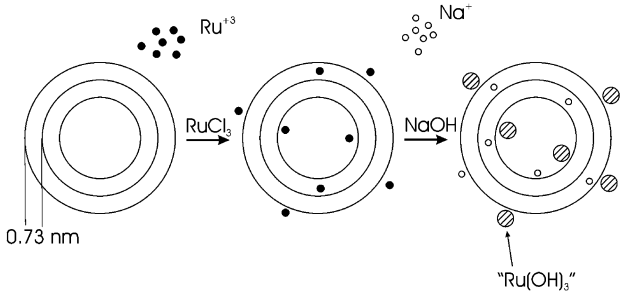

(b)

Fig. 3. Preparation of Ru(III)/TiO_2 nanotube catalysts. (a) Absorption spectra of aqueous $RuCl_3$ 10^{-4} M solution (—), mixture of $RuCl_3$ 5×10^{-5} M with colloidal TiO_2 nanotubes 10^{-3} M (Ti) after 20 min (- - -), previous mixture 20 min after addition of 0.05 M NaOH (···). The spectrum of colloidal TiO_2 nanotubes solution was subtracted from two last spectra. Colloidal solution of TiO_2 nanotubes was stabilised by 0.01 M $(C_{12}H_{25})_2(CH_3)_2NCl$. (b) Scheme of transformations: Ru ion-exchange, and formation of ruthenium hydrated oxide on the surface of TiO_2 nanotubes.

Ti/Ru = 20:1 results in decreased intensity of these two bands and the appearance of a new transition at 600 nm. The spectrum of colloidal TiO_2 nanotubes was subtracted from spectra (2) and (3) in Fig. 3a for clarity.

Addition of excess of NaOH to the colloidal solution of TiO_2 saturated with Ru^{3+} results in the shift of these two bands to the shorter wavelength region (335 and 428 nm), probably due to the formation of ruthenium-hydrated oxide, which is green in colour [4]. It should also be noted that the formation of ruthenium-hydrated oxide is less likely to occur inside the wall of nanotubes, because of the steric limitations. We believe that formation of ruthenium-hydrated oxide on both surfaces of TiO_2 nanotubes is accompanied by a leaching of ruthenium ions from the walls of the nanotubes (see Fig. 3b). At the same time, sodium ions substitute protons in TiO_2 nanotube walls [27].

Electron microscopy data are in agreement with the aforementioned mechanism of ruthenium-hydrated oxide formation outside of the TiO_2 nanotubes walls. Fig. 4 shows a TEM image of isolated TiO_2 nanotubes with deposited nanoparticles of ruthenium(III)-hydrated oxide. One can see that ruthenium nanoparticles are situated on both internal and external surfaces of the nanotubes. The average size of

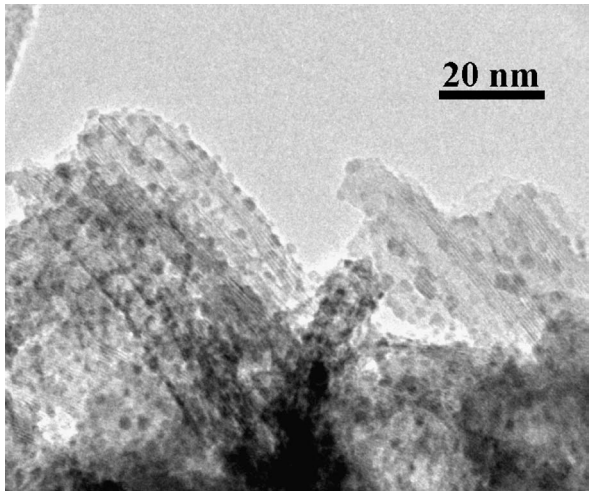

(a)

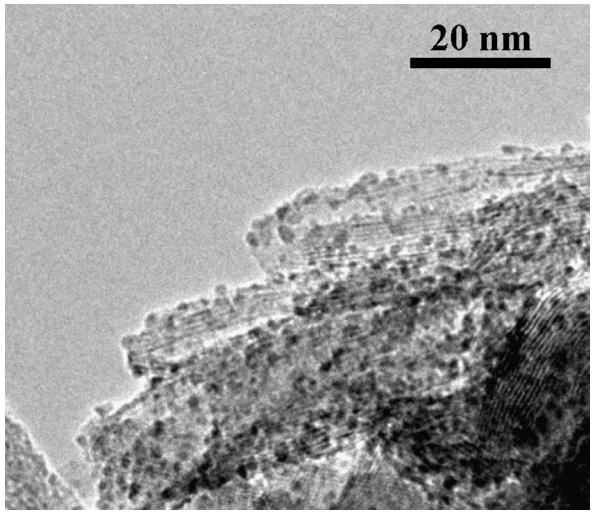

(b)

Fig. 4. TEM images of 3.3 wt% Ru(III)/TiO_2 nanotubes catalyst.

nanoparticles is 1.2–2.4 nm. The TEM image provides evidence that formation of ruthenium(III)-hydrated oxide does not occur inside the walls of nanotubes. Fig. 4a clearly shows that the multilayered structure of the wall and the distance between layers remains unchanged after deposition of ruthenium nanoparticles. Moreover, the nanoparticles are considerably larger than the space (0.72 nm) between the layers in the nanotube walls. It is interesting to note that the density of ruthenium nanoparticles on the surface of nanotubes is relatively high, reaching 0.04 nm^{-1} for 3.3 wt% ruthenium loading (see Fig. 4b). This means that a typical nanotube of 100 nm length, 4 nm i.d., and 10 nm o.d. will be decorated by >150 nanoparticles. Knowing the BET surface area of TiO_2 nanotubes, one can estimate the concentration of nanoparticles in the 3.3 wt% catalyst: 8×10^{18} nanoparticles of ruthenium-hydrated oxide in 1 g of catalyst. Based on the TEM data, we propose that an increased ruthenium loading results in an increased density of deposition of nanoparticles, rather than an increased average particle diameter. This was confirmed by the catalytic experiments.

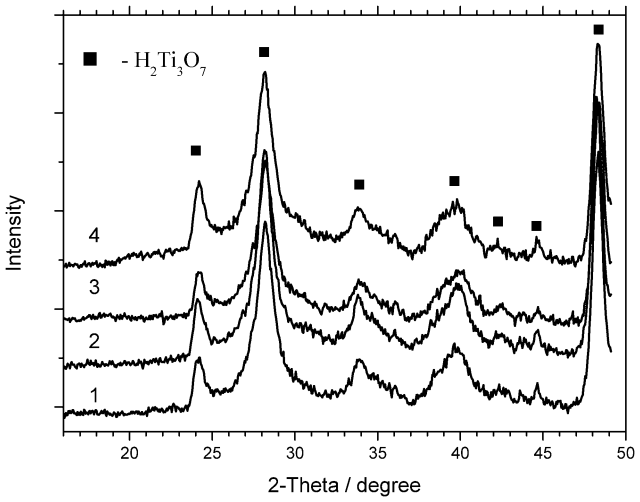

Fig. 5. XRD pattern of ruthenium(III) hydrated oxide deposited on TiO_2 nanotubes samples with different ruthenium loading: (1) 0.58, (2) 1.1, (3) 3.4, and (4) 4.6 wt%. No reflex of Ru has been found.

Crystal structure of ruthenium-hydrated oxide has not been detected in XRD spectra even at high catalyst loading, suggesting that the hydrated oxide phase is in an amorphous state (see Fig. 5), as was shown previously by others [4,29]. The crystal structure of TiO_2 nanotubes remains unchanged after deposition of ruthenium, proving that formation of ruthenium hydroxide occurs only on the surface of nanotubes. Deposition of ruthenium-hydrated oxide onto the TiO_2 nanotubes also does not change the mesoporous morphology of the support. The values of BET surface area and BJH pore volume determined by nitrogen adsorption remain ca. 200 $m^2\,g^{-1}$ and 0.7 $cm^3\,g^{-1}$, respectively. The typical BJH pore size distribution in TiO_2 nanotubes was reported previously [17]. During preparation, the nanotubular particles tend to agglomerate into secondary particles, which then form catalyst grains. The distribution of grain sizes is very broad, with the average size of about 50 μm (see Fig. 6).

3.2. Catalytic properties

The concept of a compact multichannel reactor with the millimetre-scale channel diameters and integrated functionalities of heat transfer and mixing is relatively novel and has not yet been thoroughly exploited. It was recently shown [3,28] that such a reactor is a convenient tool for studying the catalytic activity of heterogeneous catalysts in three-phase reactions, because for the relatively fast reactions such a reactor operates in the kinetic regime without any mass and heat transfer limitations over a wide range of operational conditions. Furthermore, continuous-flow nature of the reactor enables the study of kinetics of fast reactions, the dependence of reaction rate on the concentration of reagents, and catalyst deactivation.

Fig. 7 shows the dependence of the yield of benzaldehyde in the reaction of oxidation of benzyl alcohol on the oxygen flow rate at a constant liquid flow rate for the Ru(III)/TiO_2 catalysts with different Ru loadings. Benzaldehyde concentrations were measured in the outlet of the reactor. At low gas flow rates, the benzaldehyde yield depends linearly on the oxygen flow rate, with the slope corresponding to the maximum stoichiometric yield based on the amount of oxygen fed to the reactor. This suggests that below certain gas flow rates (different for different catalysts), the reaction is limited by the supply of oxygen. The greater the catalyst loading, the higher the oxygen flow rate below which a linear depen-

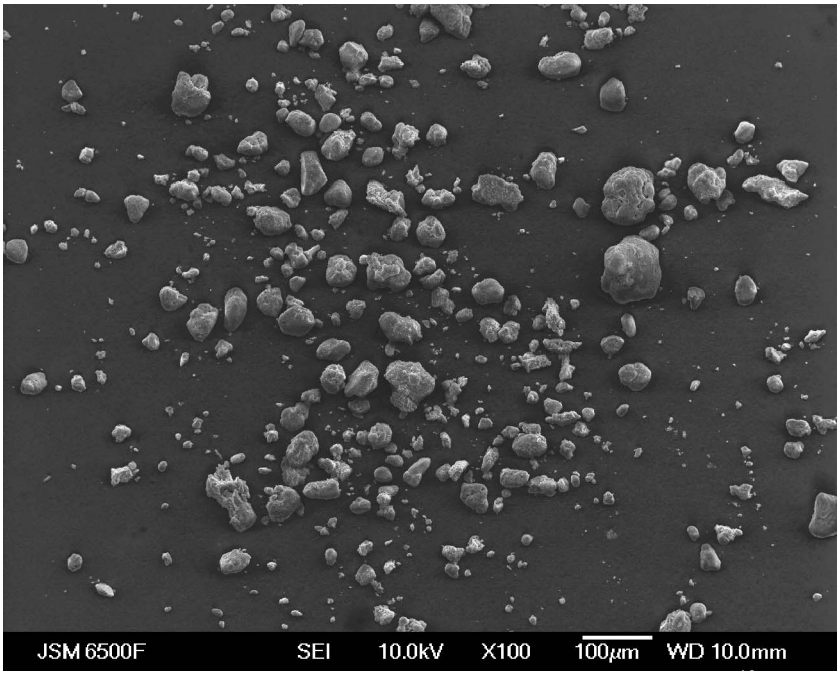

Fig. 6. Low magnification SEM image of TiO_2 nanotubes used as a support for ruthenium hydrated oxide catalyst.

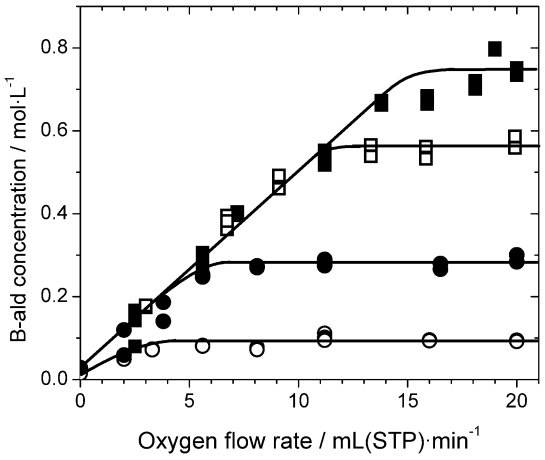

Fig. 7. Benzaldehyde concentration in the outlet of the continuous flow compact reactor as a function of the oxygen flow rate. Reactor was packed with Ru(III)/TiO_2 nanotube catalyst having different Ru loadings: (○) 0.58 wt%, (●) 1.1 wt%, (□) 2.3 wt%, (■) 3.3 wt%. Initial concentration of benzyl alcohol is 1 M, solvent is toluene, $F_l = 2$ mL min^{-1}, $P = 8$ bar, $T = 390$ K, reaction channel size 100 × 3 × 3 mm.

dence is seen. Above this critical value of oxygen flow rate, the yield is independent of the flow rate. This finding is in agreement with the mechanism of oxidation of alcohols on ruthenium-hydrated oxide catalyst, suggesting that oxidation of catalyst is not a rate-limiting step and, consequently, the observed rate of reaction has zero-order dependence on the oxygen concentration [4,29].

The maximum conversion of benzyl alcohol with 1 M initial concentration achieved in one pass through the 100 × 3 × 3 mm reactor packed with 3.3 wt% Ru(III)/TiO_2 catalyst was 75%, with very high (>99%) selectivity (see Table 1). The observed increase in the maximum conversion between 2.3 and 3.3 wt% Ru catalysts was less than the expected 1.4 times. Indeed, at high catalyst loading, the reaction rate is too high, and the effects of mass transfer may become significant. As was shown in earlier work [3], at a lower reaction rate (8.3×10^{-6} mol s^{-1}) and similar hydrodynamic conditions, the apparent reaction rate is limited by the catalyst activity. However, as shown in Fig. 7, for 3.3 wt% Ru catalyst, the 75% conversion corresponds to a higher reaction rate (2.5×10^{-5} mol s^{-1}), at which mass transfer effects may become significant.

High conversion also hinders accurate measurement of catalytic activity, because the latter depends on the reactant concentration, which is not constant along the length of a continuous plug-flow reactor. To decrease conversion, the catalysts with high loading of ruthenium were diluted with pure TiO_2 nanotubes, which were found to be inactive in the reaction of benzyl alcohol oxidation and thus would not alter the hydrodynamic regime in the reactor. The resulting effect of ruthenium loading on the activity of Ru(III)/TiO_2 nanotube catalysts in the reaction of benzyl alcohol oxidation is shown in Fig. 8. Catalysts with ruthenium loadings of 3.3, 4.6, 6.6, and 8.7 wt% were mixed with TiO_2 nanotubes in the following mass proportions: catalyst:TiO_2, 0.25, 0.2, 0.145, and 0.118. The turnover frequency (TOF) of a catalyst in a continuous flow reactor in the case of small conversion of a reactant can be calculated via the following equation [3]:

$$\mathrm{TOF} = \frac{C_{\text{b-ald}} \cdot F_{\text{l}} \cdot M_{\text{Ru}}}{m_{\text{Cat}} \cdot l_{\text{Ru}} \cdot \delta}, \qquad (2)$$

where $C_{\text{b-ald}}$ is concentration of benzaldehyde product in the outlet of reactor (M), F_{l} is the volumetric liquid flow rate

Table 1
Oxidation of various alcohols with molecular oxygen on Ru(III)/TiO_2 nanotubes and Pt/C catalysts

Catalyst	Reactant	Product	TOF[a] (h^{-1})	Selectivity[b] (%)
Ru(III)/TiO_2[c]	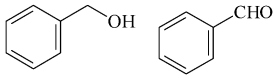		450	99.8
Ru(III)/TiO_2	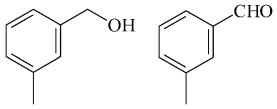		235	99.5
Ru(III)/TiO_2			128	91
Pt/C[d]	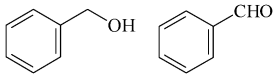		750	98.6
Pt/C	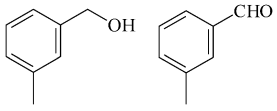		89	93.3
Pt/C			3.9	55

[a] In some cases due to the deactivation of catalyst initial TOF value is presented.
[b] Related to the benzaldehyde.
[c] 2.3 wt% ruthenium loading, experimental conditions: initial concentration of alcohol is 1 M, solvent is toluene, $F_{\text{l}} = 2$ mL min^{-1}, $P = 8$ bar, $T = 390$ K.
[d] 3.5 wt% Pt loading, experimental conditions: initial concentration of alcohol is 1 M, solvent is dioxane, $F_{\text{l}} = 2$ mL min^{-1}, $P = 8$ bar, $T = 368$ K.

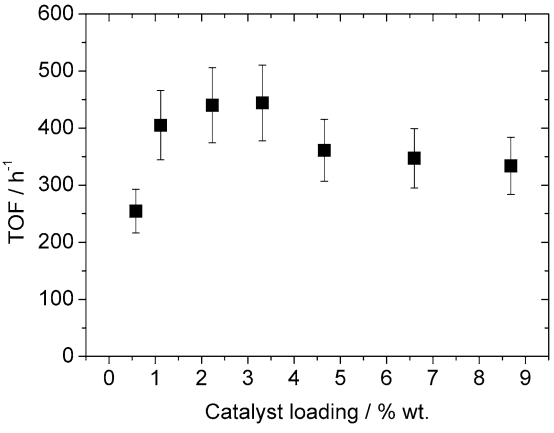

Fig. 8. The dependence of activity of Ru(III)/TiO_2 nanotube catalyst on the ruthenium loading. TOF, turnover frequency is the rate of benzyl alcohol oxidation (initial concentration 1 M) with oxygen in continues flow reactor at 390 K. For high loadings, the catalyst was "diluted" with pure TiO_2 nanotubes (see text for details).

($L\,h^{-1}$), m_{Cat} is mass of Ru(III)/TiO_2 nanotube catalyst (g), l_{Ru} is a value of ruthenium loading (%), δ is the catalyst dilution proportion, and M_{Ru} is the molar mass of ruthenium ($g\,mol^{-1}$). It should be noted that turnover number (TON) could not be defined for a continuous-flow reactor and in the absence of catalyst deactivation is equal to infinity.

Fig. 8 shows that an increase in ruthenium loading results in relatively small changes in the TOF values in the range 450–330 h^{-1}. This may be due to the retention of a high dispersion of active ruthenium on the surface of TiO_2 nanotubes over a wide range of ruthenium loadings. These catalytic test results, showing the independence of TOF on active component loading, support our argument based on the electron microscopy data, which show high dispersion and high density of Ru-hydrated oxide nanoparticles on the surface of TiO_2 nanotubes at a reasonably high 3.3 wt% loading (see Fig. 4).

The almost-constant catalytic activity of ruthenium supported on TiO_2 nanotubes could potentially be used in the preparation of structured multifunctional catalysts. For example, it has been found that using powdered Ru(III)/TiO_2 nanotube catalyst in a continuous-flow reactor results in a significant pressure drop and gradual blockage of the channels with broken-up grains of the catalyst. Preparing a structured catalyst with a durable spherical structure with TiO_2 nanotube catalyst incorporated into the large pores of the spherical support should resolve the problem of pressure drop, whereas high loading of active component onto the TiO_2 nanotubes will compensate for the dilution of Ru active sites within a grain of a structured catalyst.

It was found that Ru(III)/TiO_2 nanotube catalyst is also very active in the reactions of substituted aromatic alcohol oxidation. Table 1 compares the 2.3 wt% Ru(III)/TiO_2 nanotube catalyst and the Pt/C catalyst in the reaction of different alcohol oxidation to aldehydes using molecular oxygen. The Pt/C catalyst (Pt 3.5 wt%) was prepared by impregnating the synthetic carbon manufactured from phenolic resins (Mast Carbon, Guildford, UK) using H_2PtCl_6 as a precursor, as described previously [30]. One can see that Pt/C catalyst, active in the reaction of benzyl alcohol oxidation, has low activity and selectivity in the reactions of oxidation of substituted aromatic alcohols, whereas the Ru(III)/TiO_2 nanotube catalyst remains relatively active, having also retained high selectivity toward aldehydes. For the oxidation of thiophene 2-methanol, both catalysts exhibit relatively fast deactivation; therefore, only initial values of TOF are given in Table 1.

The problem of ruthenium(III)-hydrated oxide deactivation was discussed previously [3] for benzyl alcohol oxidation on Ru(III)/Al_2O_3 catalyst. The deactivation was caused mainly by deposition of benzoic acid (which has low solubility in toluene solvent), which could be removed by washing in aqueous alkali solution. The rate of deactivation in this case is slow (rate constant of deactivation ca. 0.018 h^{-1} [3]). In the case of ruthenium on TiO_2 nanotube catalyst, the rate of deactivation was further decreased in the presence of water in the toluene solvent; water at a saturation concentration ca. 0.7 wt% decreased the rate of deactivation in the oxidation of benzyl alcohol, whereas use of dry toluene solvent increased the rate of deactivation. These findings are in agreement with the postulate that the existence of ruthenium hydroxo species is crucial for catalytic activity [29]. The fact that the rate of catalyst deactivation in the reaction of benzyl alcohol oxidation dissolved in toluene saturated with water is almost zero also suggests that leaching of ruthenium and particle sintering during the reaction is negligible.

In the case of oxidation of the sulphur-containing alcohol, the mechanism of deactivation appears to be different. The observed rate of catalyst deactivation is much higher (0.66 h^{-1}) than in the case of deactivation in the reaction of benzyl alcohol oxidation, and deactivated catalyst does not recover activity after washing with a solution of NaOH. This is likely due to the irreversible formation of ruthenium sulphide species.

4. Conclusions

A ruthenium(III)-hydrated oxide catalyst supported onto the mesoporous TiO_2 nanotubes was prepared by ion exchange followed by alkali treatment. The effective ion-exchange properties of TiO_2 nanotubes provide a high capacity for ruthenium ions, resulting in high catalyst loading with even distribution of small catalyst nanoparticles. The ruthenium-hydrated oxide nanoparticles are 1–2 nm in size, and the density of the particles on the surface of TiO_2 nanotubes can reach 0.04 nm^{-2}. The catalyst nanoparticles decorate both the internal and external surfaces of the nanotubes and are not found between the layers of the multilayered nanotube walls.

The activity of catalysts was studied in the reaction of selective oxidation of alcohols with oxygen in a continuous-flow multichannel compact reactor. The catalyst showed high activity (e.g., for the catalyst with Ru loading 3.3 wt%, TOF $\leqslant$ 450 h^{-1}, at 390 K, 1 M feed benzyl alcohol concentration and 75% conversion during a single pass through the reactor), high selectivity (99.8%), and good stability. It was found that the specific catalytic activity (TOF) could be maintained at a high value over a wide range (0.5–9 wt%) of ruthenium loading. The independence of activity from catalyst loading is attributed to the high dispersion of deposited ruthenium-hydrated oxide in the catalysts with high loading, which was confirmed by the microscopy studies. The catalysts performed well in the reaction of substituted aromatic alcohol oxidation.

Acknowledgments

This work was funded through EC project “CREATION” G5RD-CT-2002-00724. The authors are grateful to collaborators on the project, F. Kapteijn (Technische Universiteit

Delft), M. Besson (Institut de Recherches sur la Catalyse, Lyon), S. Tennison (Mast Carbon Ltd.), and M. Coleman and P. Ravenscroft (GlaxoSmithKline), for the many useful discussions.

References

[1] T. Mallat, A. Baiker, Chem. Rev. 104 (2004) 3037.
[2] G. Dummann, U. Quittmann, L. Groschel, D.W. Agar, O. Worz, K. Morgenschweis, Catal. Today 79–80 (2003) 433.
[3] D.V. Bavykin, A.A. Lapkin, S.T. Kolaczkowski, P.K. Plucinski, Appl. Catal. A 288 (2005) 175.
[4] K. Yamaguchi, N. Mizuno, Chem. Eur. J. 9 (2003) 4353.
[5] K. Yamaguchi, N. Mizuno, Angew. Chem. Int. Ed. 41 (23) (2002) 4538.
[6] K. Yamaguchi, K. Mori, T. Mizugaki, K. Ebitani, K. Kaneda, J. Am. Chem. Soc. 122 (2000) 7144.
[7] Z. Opre, J.-D. Grunwaldt, M. Maciejewski, D. Ferri, T. Mallat, A. Baiker, J. Catal. 230 (2005) 406.
[8] T. Kasuga, M. Hiramatsu, A. Hoson, T. Sekino, K. Niihara, Langmuir 14 (1998) 3160.
[9] X. Sun, Y. Li, Chem. Eur. J. 9 (2003) 2229.
[10] Z.Y. Yuan, B.L. Su, Colloids Surf. A: Physicochem. Eng. Aspects 241 (2004) 173.
[11] C.C. Tsai, H. Teng, Chem. Mater. 16 (2004) 4352.
[12] C.H. Lin, S.H. Chien, J.H. Chao, C.Y. Sheu, Y.C. Cheng, Y.J. Huang, C.H. Tsai, Catal. Lett. 80 (3–4) (2002) 153.
[13] V. Idakiev, Z.-Y. Yuan, T. Tabakova, B.-L. Su, Appl. Catal. A 281 (2005) 149.
[14] C.H. Lin, C.H. Lee, J.H. Chao, C.Y. Kuo, Y.C. Cheng, W.N. Huang, H.W. Chang, Y.M. Huang, M.K. Shih, Catal. Lett. 98 (1) (2004) 61.
[15] J.C. Xua, M. Lua, X.Y. Guob, H.L. Lia, J. Mol. Catal. A 226 (2005) 123.
[16] J.J. Yang, Z.S. Jin, X.D. Wang, W. Li, J.W. Zhang, S.L. Zhang, X.Y. Guo, Z.J. Zhang, Dalton Transact. 20 (2003) 3898.
[17] D.V. Bavykin, V.N. Parmon, A.A. Lapkin, F.C. Walsh, J. Mater. Chem. 14 (2004) 3370.
[18] D.V. Bavykin, S.N. Gordeev, A.V. Moskalenko, A.A. Lapkin, F.C. Walsh, J. Phys. Chem. B 109 (2005) 8565.
[19] J. Hong, J. Cao, J. Sun, H. Li, H. Chen, M. Wang, Chem. Phys. Lett. 380 (2003) 366.
[20] T. Kasuga, M. Hiramatsu, A. Hoson, T. Sekino, K. Niihara, Adv. Mater. 11 (15) (1999) 1307.
[21] Q. Chen, G.H. Du, S.L.M. Zhang Peng, Acta Crystallogr. B 58 (2002) 587.
[22] D.C. Harris, Quantitative Chemical Analysis, sixth ed., Freeman, New York, 2003.
[23] F.A. Cotton, G. Wilkinson, Advanced Inorganic Chemistry a Comprehensive Text, Interscience, New York, 1962.
[24] E.A. Seddon, K.R. Seddon, The Chemistry of Ruthenium, Elsevier, Amsterdam, 1984, p. 1373.
[25] D.R. Lide, Handbook of Chemistry and Physics, CRC, Boca Raton/London, 2004.
[26] S.K. Shukla, J. Chromatogr. 8 (1962) 96.
[27] M. Zhang, Z. Jin, J. Zhang, X. Guo, J. Yang, W. Li, X. Wang, Z. Zhang, J. Mol. Catal. A 217 (2004) 203.
[28] P.K. Plucinski, D.V. Bavykin, S.T. Kolaczkowski, A.A. Lapkin, Catal. Today (2005), 10.1016/j.cattod.2005.06.021.
[29] T.L. Stuchinskaya, M. Musawir, E.F. Kozhevnikova, I.V. Kozhevnikov, J. Catal. 231 (2005) 41.
[30] H.E. van Dam, H. van Bekkum, J. Catal. 131 (1991) 335.